Scientia Iranica A (2020) 27(3), 1050–1065

SCIENTIA IRANICA

Sharif University of Technology
Scientia Iranica
Transactions A: Civil Engineering
http://scientiairanica.sharif.edu

Modified seismic design lateral force distribution for the Performance-Based Plastic Design (PBPD) of steel moment structures considering soil flexibility

A. Gholamrezatabar[a], B. Ganjavi[b], G. Ghodrati Amiri[a,*], and M.A. Shayanfar[a]

a. *School of Civil Engineering, Iran University of Science & Technology, Narmak, Tehran, P.O. Box 16765-163, Iran.*
b. *Department of Civil Engineering, University of Mazandaran, Babolsar, Iran.*

Received 25 May 2017; received in revised form 21 November 2017; accepted 18 August 2018

KEYWORDS
Seismic design lateral force;
Performance-based plastic design;
Steel moment structures;
Soil-structure interaction;
Optimum shear proportion factor.

Abstract. It is well known that structures designed by conventional seismic design codes experience large inelastic deformations during strong ground motions. A realistic estimation of force distribution based on inelastic response is one of the important steps in a comprehensive seismic design methodology in order to represent expected structural responses more accurately. This paper presents an extensive parametric study to investigate the structural damage distribution along the height of the Steel Moment-Resisting Frames (SMRFs) designed based on the state-of-art constant-ductility Performance-Based Plastic Design (PBPD) approach considering soil flexibility effects when subjected to 20 strong ground motions. To this end, the effects of fundamental period, target ductility demand, and base flexibility level are investigated and discussed. Based on the numerical results of this study, simplified equations are proposed for practical purposes to refine and modify the lateral force distribution pattern already suggested by researchers based on the study of inelastic behavior developed for fixed- and flexible-base structures by using relative distribution of maximum story shears of the selected structures subjected to various earthquake ground motions. It is demonstrated that the proposed equations can adequately estimate the optimum values of the shear proportioning factor in both fixed-base and soil-structure systems.

1. Introduction

The design lateral forces and design story shears from the equivalent lateral force recommended by the current code-specified seismic design procedure (e.g., IBC 2009 [1], ASCE/SEI 7–10 [2], NEHRP 2009 [3], UBC [4]) are primarily based on elastic analysis. In this method, the structural elements are designed based on equivalent static forces, and the shape of the fundamental mode of the structure is dominant to determine the height-wise distribution of these seismic design static forces. Establishing such code-compliant lateral load distributions patterns may not provide an accurate representation of the story shear strength demands and explicitly lead to seismic performance assessment criteria [5–12]. Chopra [13] conducted the nonlinear dynamic analysis of several shear-building models subjected to the El-Centro Earthquake of 1940 to evaluate the ductility demands corresponding to each story. The models were designed in accordance with the seismic force patterns specified by Uniform

*. *Corresponding author.*
E-mail addresses: gholamrezatabar@iust.ac.ir (A. Gholamrezatabar); b.ganjavi@umz.ac.ir (B. Ganjavi); ghodrati@iust.ac.ir (G. Ghodrati Amiri); Shayanfar@iust.ac.ir (M.A. Shayanfar)

doi: 10.24200/sci.2019.21616

Building Code [4]. It was concluded that this distribution pattern did not lead to equal ductility demand in all stories. Moghaddam [14] conducted the same analysis of a number of shear buildings with the specified yield strength distributed by UBC-97 [4] suggestion pattern. They showed that the code-compliant lateral load distribution did not lead to a uniform height-wise distribution of ductility. Moghaddam and Mohammadi [15] proposed a design lateral load pattern for the seismic design of shear-building structures to achieve uniform deformation distribution. In another investigation, they developed a new concept to optimize the distribution pattern for the performance-based seismic design approach [11]. However, their study was based on the results of shear-building structures that might not be applicable to more realistic building structures such as moment-resisting frames that are basically designed based on the "strong-column weak-beam" design philosophy. Several other studies focused on moment-resisting frame that aimed to develop new lateral load patterns to control the amount of the global structural damage and to achieve predefined performance objectives and, finally, provide higher performance levels exposed to seismic ground motions. Leelataviwat et al. [8] proposed improved load distribution using the concept of energy balance applied to moment-resisting frames with an intended yield mechanism. Lee and Goel [16] primarily discussed the discrepancy between the earthquake-induced shear forces and the forces determined by lateral load distribution patterns. They applied the same concept to propose load pattern in accordance with the Uniform Building Code [4], which was a function of the mass and fundamental period of the structure. Goel et al. [17] applied the method successfully to a variety of common steel framing systems and reinforced concrete Moment Frames (MFs). Through the results of extensive inelastic static and dynamic analyses, they showed that the frames could develop desired strong column-sway mechanisms and that the story drifts and ductility demands were well within the target values, thus meeting the desired performance objectives. Park and Medina [18] proposed a seismic design methodology for moment-resisting frames based on uniform structural damage distributed along the height. They concluded that, based on the proposed approach, designs were expected to provide increased protection against global collapse and loss of life during a strong earthquake event. Chao et al. [19] primarily reviewed the lateral force distributions used in the current seismic codes by conducting the nonlinear dynamic analysis of several frame structures. They demonstrated that code lateral force distributions did not represent the maximum force distributions that might be induced during the nonlinear response of motions and might make inaccurate predictions of deformation and force demands. Their comprehensive studies lead to the development of a new seismic design lateral load distribution based on the inelastic behavior of a structure and, also, a new methodology called Performance-Based Plastic Design (PBPD) for the seismic design of a wide range of frame systems including moment-resisting frames, eccentrically-braced frames, special truss-moment frames, and reinforced concrete frames. In these investigations, performance limit states are pointed out by the predictable global yield mechanism and the pre-designated target drift limit. The design base shear at each performance level is derived from an energy-based method, where the energy required to push the structure up to the target drift is calculated as a fraction of elastic input energy that is obtained from the selected elastic design spectra [16,17,19]. However, they did not incorporate the target ductility demand in the design process directly.

All of the above-mentioned research studies are based on the fixed-base structures without considering the effect of soil flexibility, i.e., Soil-Structure Interaction (SSI). Several studies have been performed to investigate the effect of SSI on the seismic responses of structures [20–24]. The results of these studies demonstrated that structures supported by soil-foundation might be affected by SSI significant roles due to wave propagation in the soil medium. Based on the concept developed for fixed-base shear structures, Ganjavi and Hao [25] proposed new optimum design lateral loading patterns for the seismic design of elastic soil-structure systems through the intensive dynamic analysis of multistory shear-building models subjected to a group of 21 artificial earthquakes adjusted to the soft soil design. Ganjavi et al. [26] also parametrically investigated the adequacy of code-specified lateral loading patterns for the seismic design of elastic and inelastic soil-structure systems based on the analysis of shear buildings considering SSI effects. Due to the challenges of code-specified lateral load distributions and the need to improve the seismic performance of flexible-base buildings on soft soils, they [26] proposed an optimum seismic design methodology for nonlinear shear buildings located on soft soils based on the concept of uniform damage distribution. However, their study was also based on the results of shear building structures that might not be applicable to more realistic building structures such as SMRFs.

This study evaluates lateral force distributions by the nonlinear dynamic analysis of constant-ductility SMRF structures designed according to the PBPD procedure located on alluvium soil considering SSI effects. The aim of this study is to parametrically investigate height-wise structural damage (ductility demand) distribution designed based on the conventional PBPD approach for constant-ductility fixed- and flexible-base SMRF structures. Moreover, the adequacy of load patterns already proposed in PBPD is investigated through the height-wise distribution of the inter-story ductility demand ratio subjected to various strong ground motions.

2. Analytical model based on PBPD approach

The PBPD method is based on two key performance limit sates including pre-selected target drift and yield mechanisms [8]. These two design parameters control the degree and distribution of structural damages directly. In this approach, the determination of design base shear, lateral force distribution, and plastic design corresponding to the specified performance level are the three main components of design. For a specified hazard, the design base shear is calculated by equating the work needed to push the structure monotonically up to the target drift to the energy required by an equivalent Elastic-Plastic Single-Degree-Of-Freedom (EP-SDOF) system to achieve the same state. Moreover, the height-wise distribution of lateral design forces is developed based on the concept of the relative story shear distributions and is consistent with the results of the inelastic dynamic response [19]. Finally, the proposed plastic design procedure is performed to detail frame members in order to achieve the intended yield mechanism.

2.1. Design base shear

As explained earlier, the design base shear as a key element in the PBPD method is calculated by equating the work needed to push the structure monotonically up to the target drift to that required by an equivalent EP-SDOF system to achieve the same state. For idealized Elastic-perfect Plastic (EP) behavior and using the value of pseudo-velocity or substituting pseudo-acceleration, the work energy can be calculated through Eq. (1) [27]:

$$E_e+E_p=\gamma E=\gamma(1/2MS_v^2)=\frac{1}{2}\gamma M\left(\frac{T}{2\pi}S_a.g\right)^2, \quad (1)$$

where E_e and E_p are the elastic and plastic components of the energy needed to push the structure up to the target drift, respectively. S_v is the design pseudo-spectral velocity; S_a is the pseudo-spectral acceleration; T and M are the natural period and total mass of the system, respectively. γ is the energy modification factor, which is related to the structural ductility factor (μ_s) and the ductility reduction factor (R_μ), and can be obtained by the following equation:

$$\gamma=\frac{2\mu_s-1}{R_\mu^2}. \quad (2)$$

Based on the spectra proposed by Newmark and Hall

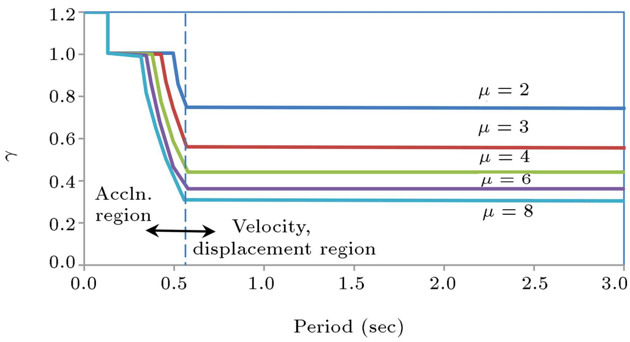

Figure 1. Energy modification factor, γ, versus the period.

(1982) [27], the energy modification factor (γ) can be obtained through Eq. (2), as shown in Figure 1 [16].

The work-energy equation can be rewritten in the following form:

$$\frac{1}{2}\left(\frac{W}{g}\right)\times\left(\frac{T}{2\pi}\times\frac{V_y}{W}g\right)^2+V_y\left(\sum_{i=1}^{N}\lambda_i h_i\right)\theta_p$$
$$=\frac{1}{2}\gamma\left(\frac{W}{g}\right)\times\left(\frac{T}{2\pi}S_a g\right)^2. \quad (3)$$

By simplifying Eq. (3), the ratio of (V_y/W) can be written through Eq. (4):

$$\frac{V_y}{W}=\frac{-\alpha+\sqrt{\alpha^2+4\gamma S_a^2}}{2}, \quad (4)$$

where α is a dimensionless parameter given by Eq. (5):

$$\alpha=\left(h^*\times\frac{\theta_P 8\pi^2}{T^2 g}\right), \quad (5)$$

where θ_p represents the plastic rotation at the target drift ratio, and h^* stands for $\sum_{i=1}^{N}\lambda_i h_i$, where λ_i is the proportioning factor of the equivalent lateral force at level i.

2.2. Lateral force distribution

A new design lateral force distribution for the plastic design was obtained based on the results of inelastic dynamic responses and maximum story shears along the height of structural systems, defined as Eq. (6) [19]:

$$V_i=\left(\frac{\sum_{j=i}^{n}w_j h_j}{\sum_{j=1}^{n}w_j h_j}\right)^{0.75T^{-0.2}}V_y, \quad (6)$$

where w and h are the seismic weight and height above the base, respectively. T is the fundamental period and V_y represents the design base shear. The equation is more consistent with the results of inelastic analysis than with the code-specified seismic load pattern. It can be shown that the ratio V_i/V_n, designated as shear distribution factor, β_i, can be obtained through Eq. (7) [19]:

$$\frac{V_i}{V_n} = \beta_i = \left(\frac{\sum_{j=i}^{n} w_j h_j}{w_n h_n} \right)^{0.75T^{-0.2}}, \tag{7}$$

where V_i and V_n are the story shear at level i and top level, respectively, and β_i is the shear proportioning factor at level i. Hence, the lateral force at level i, F_i, can be expressed as:

$$F_i = (\beta_i - \beta_{i+1}) V_n. \tag{8}$$

2.3. Plastic design procedure

The provided design approach is capable of achieving the satisfactory performance of structures under a severe earthquake by means of a pre-defined controlled mechanism. The procedure develops a strong-column-weak beam mechanism and a stable hysteretic response within an acceptable margin of target drift [8]. By applying the principle of virtual work for the beam mechanism (Figure 2), the required beam strength at each level can be obtained through Eq. (9):

$$\sum_{i=1}^{n} 2\beta_i M_{pbr} + 2M_{pc} = \sum_{i=1}^{n} F_i h_i = \sum_{i=1}^{n} (\beta_i - \beta_{i+1}) h_i F_n, \tag{9}$$

where M_{pbr} and M_{pc} are the plastic moment of beams and the required plastic moment of columns in the first story, respectively (Figure 2). Leelataviwat et al. [8] proposed the plastic moment of the first-story columns to avoid the pre-defined mechanism as in Eq. (10):

$$M_{pc} = \frac{1.1 V h_1}{4}, \tag{10}$$

where V is the total base shear, h_1 is the height of the first story, and coefficient 1.1 is the overstrength factor to account for possible overloading due to strain hardening. However, as the main goal of this approach, an attempt has been made to prevent the formation of plastic hinges in the columns except at the column bases of the structure. Hence, the column should be designed for the flexural moment greater than the sum of the flexural strength of the beams at the same joint. To ensure that the strong column-weak beam mechanism is achieved, columns should be designed for the sum of the nominal plastic moment of beams multiplied by the over-strength factor (ξ). Moreover, to include the beams yielding overstrength, the applied force at each level, F_i, must be updated as follows (Eq. (11)):

$$F_{iu} = (\beta_i - \beta_{i+1}) F_{nu}, \tag{11}$$

where F_{nu} is the updated force at the roof level and can be determined by the equilibrium equation for one column as Eq. (12):

$$\sum_{i=1}^{n} (\beta_i - \beta_{i+1}) h_i F_{nu} = M_{pc} + \sum_{i=1}^{n} \xi_i M_{pbi}, \tag{12}$$

where M_{pc} is the plastic moment at the base of the frame (Eq. (10)), and ξ and M_{pbi} are the overstrength factor and the nominal plastic moment of beam at level i, respectively. After updating the lateral forces, design moments of the column can be determined by developing the column as a cantilever based on Eq. (13):

$$M_c(h) = \sum_{i=1}^{n} \delta_i \xi_i M_{pbi} - \sum_{i=1}^{n} \delta_i F_{iu} (h_i - h), \tag{13}$$

where $M_c(h)$ is the moment in the column at height h above the ground, and δ_i is equal to 1 for $h \leq h_i$ and zero for else. The axial force in the column at height h above the ground, $P_c(h)$, can be obtained through Eq. (14):

$$P_c(h) = \sum_{i=1}^{n} \frac{2\xi_i M_{pbi}}{L} + P_{cg}(h), \tag{14}$$

where L is the span length of the beams, and $P_{cg}(h)$ is the gravity axial force acting at height h. By applying the explained approach, the values of $M_c(h)$ and $P_c(h)$ of the column element can be obtained according to the plastic analysis procedure and, then, it can be designed as a beam-column element by appropriate

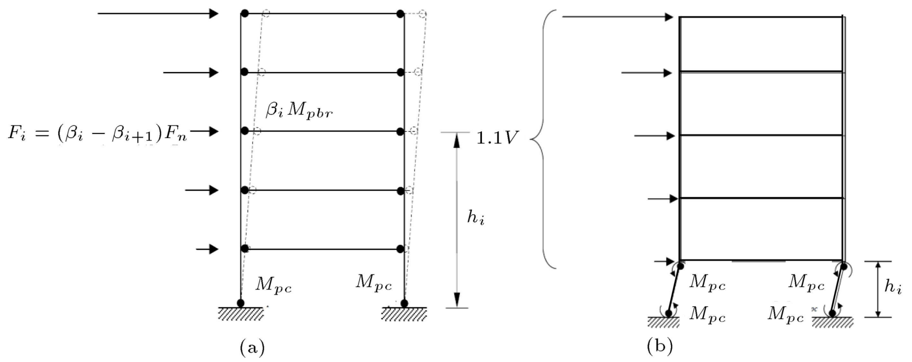

Figure 2. One-bay frame with (a) selected mechanism and (b) frame with soft-story mechanism.

Table 1. Design parameters for 4-, 8-, 12-, 16-story steel Performance-Based Plastic Design (PBPD) frames used to calibrate β_i.

Design parameters	**10% in 50 years hazard**	**Story height and beam span for single-bay moment-resisting frames**
Number of Stories	4, 8, 12, 16	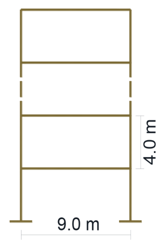
S_a	0.36 g	
Yield drift ratio θ_y	1%	
Target drift ratio θ_u	2%, 4%, 6%	
Inelastic drift ratio $\theta_p = \theta_u - \theta_y$	1%, 3%, 5%	
$\mu = \theta_u / \theta_y$	2, 4, 6	
$R\mu$	2, 4, 6	
γ	0.75, 0.438, 0.306	
$\beta_i = \left(\frac{V_i}{V_n}\right)^b$	$b = 0.75T^{-0.2}$	

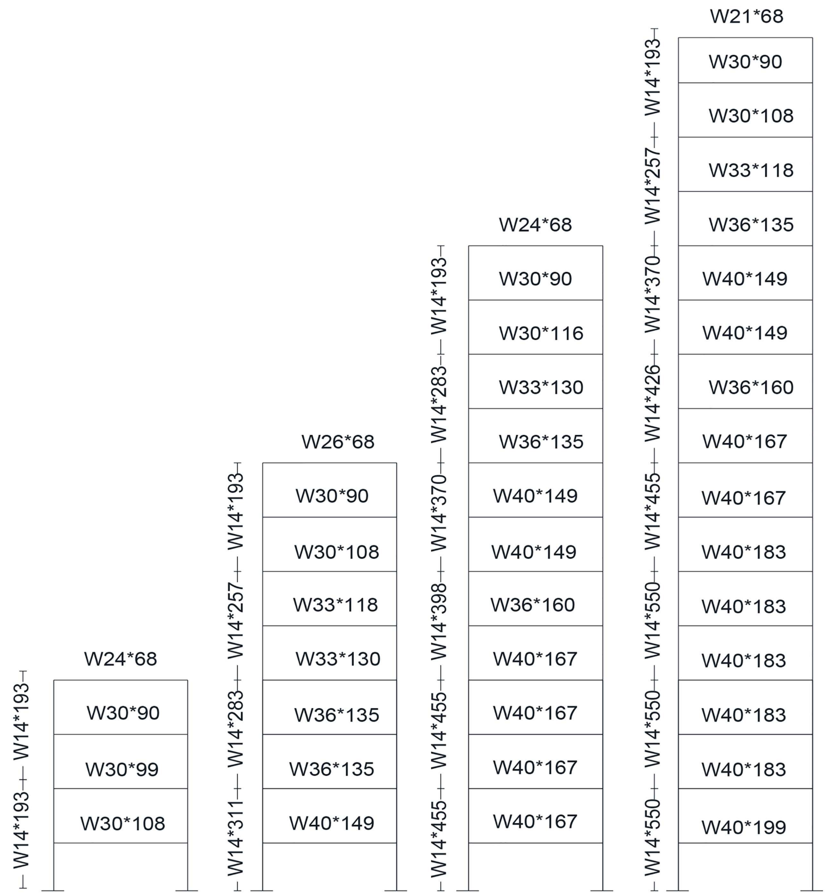

Figure 3. Selected 4-, 8-, 12-, 16-story moment frames.

design provisions. Finally, it should be mentioned that, as a well-known numerical modeling strategy, the superstructure frame elements followed the lumped-plasticity modeling approach to computing their non-linear response regarding the Rayleigh damping and rigid diaphragm assumption. For computer modeling, beams and columns were modeled as non-degrading quasi-elastoplastic (i.e., at a strain-hardening ratio of 2%). A moment-curvature relationship that considers the axial load-flexural bending interaction was considered to model the hysteretic behavior of the steel columns. However, slab contribution to the beam's bending capacity was neglected in this study. The design parameters and elevation views of designed MFs based on PBPD approaches are listed in Table 1. The sizes of beams and columns were selected using AISC-LRFD specifications [28] assuming A572 GR.50 steel for all members, as shown in Figure 3.

3. Base flexibility model

In this study, a cone model was proposed to simulate the dynamic behavior of an elastic homogeneous soil half-space, as shown in Figure 4 [29]. The model is developed using one-dimensional wave propagation theory and can represent a circular rigid foundation with mass m_f and mass moment of inertia I_f resting on homogeneous half-space soil. The cone model is widely used for modeling both surface and embedded foundations and, in lieu of the rigorous elasto-dynamical approach, it can provide sufficient accuracy for engineering design purposes [30]. The soil-foundation system is modeled by an equivalent linear discrete model based on the cone model approach with frequency-dependent coefficients [29]. The foundation is considered as a circular rigid disk (the flexibility of the foundation is not taken into account). The components of motions for the following half-space were modeled through two transitional and rotational Degree Of Freedoms (DOFs). The coefficient of sway and rocking springs and dashpots representing the associated motions are summarized as in Eqs. (15) and (16) [29]:

$$k_h = \frac{8\rho V_s^2 r}{2-\upsilon}, \qquad c_h = \rho V_s A_f, \tag{15}$$

$$k_\varphi = \frac{8\rho V_s^2 r^3}{3(1-\upsilon)}, \qquad c_\varphi = \rho V_p I_f,$$

$$M_\varphi = \frac{9\pi \rho r^5}{128}(1-\upsilon)\left(\frac{V_p}{V_s}\right)^2, \tag{16}$$

where k_h, k_φ, c_h, and c_φ are the sway stiffness, sway viscous damping, rocking stiffness, and rocking viscous damping, respectively. ρ, υ, V_p, and V_s stand for the density, Poisson's ratio, and dilatational and shear wave velocities of soil, respectively, and r is the radius of the equivalent circular foundation. Moreover, for the vertical and rocking motions in the case of nearly incompressible soil ($1/3 < \upsilon < 1/2$), an additional tramped mass moment of inertia ΔM_φ equal to $\Delta M_\varphi = 0.3\pi(\upsilon - 1/3)\rho r^5$ is added to I_f, which is connected to the foundation and moves as a rigid body in the phase with the foundation for the rocking degree of freedom. An internal rotational DOF φ, with a mass moment of inertia m_φ, was defined to incorporate frequency dependency of soil dynamic stiffness. It is worth noting that, based on the current seismic provisions such as NEHRP 2003 [3] and FEMA 440 [31], the soil strain level related to the degraded shear wave velocity to approximate the soil nonlinearity effects on soil-foundation elements is considered [32].

It is shown that, for a specific earthquake, the seismic response of a soil-structure system depends on the dynamic characteristics of the structure and soil beneath it. The SSI effective parameters that are known as non-dimensional key parameters and can best describe the seismic response of the superstructure in a complex soil-structure system are defined as follows [33].

A dimensionless frequency as an index for the structure-to-soil stiffness ratio is defined as $a_0 = \omega_{fix}\bar{H}/v_s$, where ω_{fix} denotes the natural frequency of the fixed-base structure. $\bar{H}$ is the effective height of the structure corresponding to the fundamental mode properties of Multi-Degree Of Freedom (MDOF)

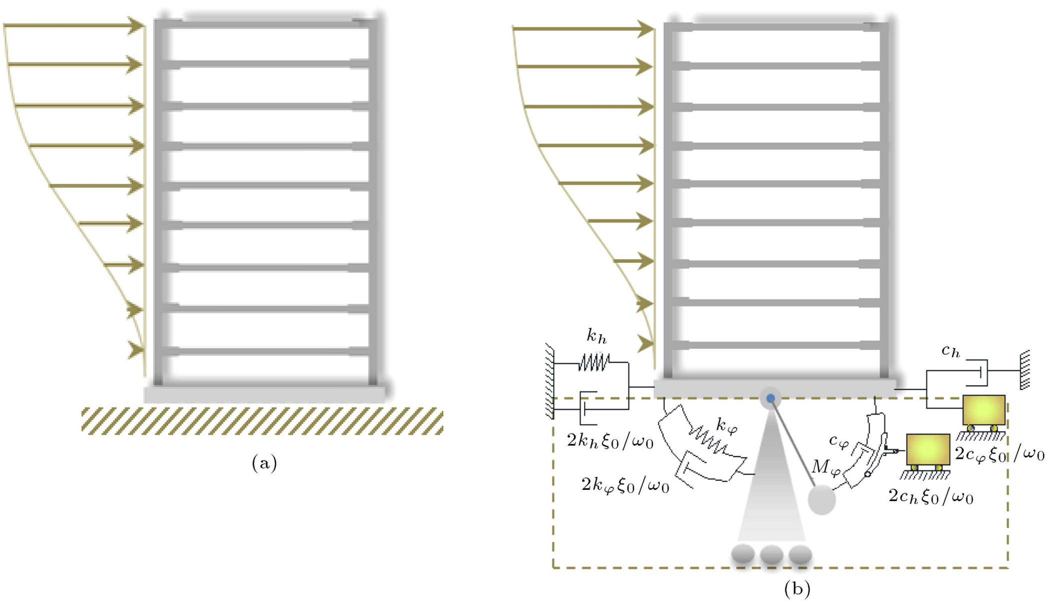

Figure 4. Typical multi-story Steel Moment-Resisting Frame (SMRF) building models: (a) Fixed-base model and (b) flexible-base model.

building and can be obtained through Eq. (17):

$$\bar{H} = \sum_{j=1}^{n} \left[m_j \varphi_{j1} \left(\sum_{i=1}^{j} h_i \right) \right] \Big/ \sum_{j=1}^{n} m_j \varphi_{j1} \ , \tag{17}$$

where j is the number of stories, m_j is the mass of the jth story, h_i is the height from the base level to level j, and φ_{j1} is the amplitude at the jth story of the first mode.

It is shown that a_0 has the most significant effects on the seismic response of the soil-structure system [34]. Based on studies conducted to categorize the intensity of the soil-structure interaction effects due to the base flexibility, a_0 takes the value between zero for fixed-base structures and 2 for the very flexible-base models [35].

- Aspect ratio of the building $\bar{H}/r$ is defined as the second interacting parameter with various effects on SSI practices [35];
- Ductility demand of structure is defined as $\mu = u_m/u_y$, where u_m and u_y are the maximum inter-story displacement and the yield inter-story displacement, respectively [36];
- Structure-to-soil mass ratio index is defined as $\bar{m} = m_{tot}/\rho r^2 H$, where m_{tot} and H are the total weight and total height of the structure, respectively;
- The ratio of the foundation-to-structure mass is m_f/m_{tot}, where m_f is the mass of the rigid foundation;
- Material damping ratio of the soil (ξ_0).

The first two interacting parameters are the key parameters that define the main SSI effect [31]. The third one controls the level of nonlinearity in the structure. Other parameters of less importance are assigned to some typical values for conventional building structures [35]. Hence, this study considers the foundation-to-structure mass ratio as 0.5 and the foundation mass ratio as %10 of the total mass of the superstructure. Poisson's ratio is set to 0.4 for the alluvium soil. In addition, the damping ratio of the soil material is set to 5%.

4. Nonlinear dynamic analysis procedure and selected ground motions

A series of 4-, 8-, 12-, and 16-story Steel Moment-Resisting Frames (SMRFs) are considered to investigate the effect of various design load patterns on the height-wise distribution of story shear forces. All models are incrementally subjected to a group of strong ground motions, and a step-by-step solution scheme is applied during time history analysis. The steel frames were analyzed based on the nonlinear dynamic analysis via computer software OpenSees [37]. Rayleigh-type damping was considered for the analysis, in which 5% of critical damping was assigned to the first two modes of vibration of the frames. Further, nonlinear static (pushover) analyses for each frame were performed to obtain relevant dynamic characteristics such as base shear and roof drift at the first plastic hinge and yielding. It should be noted that pushover analysis was conducted by the OpenSees software [37], considering a slow ramp loading function and a triangular-inverted loading distribution as prescribed in the Mexican seismic design standards, similar to that of the ASCE-7-10 load pattern (2010) and utilized by Ruiz-García and González for steel MF structures [38]. Since the objective of this study is to achieve a pre-specified constant-ductility demand, it is necessary to evaluate the nonlinear maximum story drift demand for various building frames. Hence, it was decided to scale up the acceleration spectral ordinates such that the maximum inter-story ductility demand among all stories reached the specified target value [38]. For the inelastic dynamic analysis, an ensemble of 20 earthquake ground motions with different characteristics was utilized to incorporate the effect of ground motion characteristics recorded on alluvium (NEHRP site class D [39]). All the selected ground motions are obtained from earthquakes at a magnitude greater than 6.5 having the closest distance to fault rupture more than 10 km without pulse-type characteristics. The main parameters of the selected ground motions are given in Table 2. For each record, the horizontal component with a larger peak ground velocity is defined as a strong component. A flow chart is provided to show iterative analysis procedures for the constant-ductility PBPD approach, as illustrated in Figure 5 [40].

5. Relative story shear distribution

The relative story shear distribution is defined as the ratio of maximum earthquake-induced story shear force at level i to that at top level n (i.e., $\beta = V_i/V_n$). The mean responses are obtained by averaging the results of the structures to each record. It is notable that story shear V_x in any story is the sum of the lateral forces above that story; thus, the story shear distribution and lateral force distribution have a direct relationship defined as Eq. (18):

$$V_x = \sum_{i=x}^{n} F_i. \tag{18}$$

In addition, the proposed equation (Eq. (18)) tends to somewhat overestimate the optimal b value obtained from the analyses. Eq. (19) is recommended and used for both cases of fixed- and flexible-base SMRFs as follows:

$$\beta_i = (V_i/V_n)^b. \tag{19}$$

Table 2. Characteristics of strong ground motions used in this study.

Event	Record ID	Station name	Mag.	Distance (km)	A_g (g)	V_g (cm/s)	D_g (cm)
1	RSN68.eq	LA - Hollywood Stor FF	6.61	22.8	0.2	21.7	15.9
2	RSN162.eq	Calexico Fire Station	6.53	10.5	0.3	22.5	9.9
3	RSN169.eq	Delta	6.53	22.0	0.3	33	20.2
4	RSN174.eq	El Centro Array #11	6.53	12.6	0.4	44.6	21.3
5	RSN721.eq	El Centro Imp. Co. Cent	6.54	18.2	0.4	48.1	19.3
6	RSN728.eq	Westmorland Fire Station	6.54	13.0	0.2	32.3	22.3
7	RSN752.eq	Capitola	6.93	15.2	0.5	38	7.1
8	RSN776.eq	Hollister - South & Pine	6.93	27.9	0.4	63	32.3
9	RSN777.eq	Hollister City Hall	6.93	27.6	0.2	45.5	28.5
10	RSN778.eq	Hollister Differential Array	6.93	24.8	0.3	44.2	19.7
11	RSN783.eq	Oakland - Outer Harbor Wharf	6.93	74.2	0.29	41.8	9.6
12	RSN953.eq	Beverly Hills - 14145 Mulhol	6.69	17.2	0.5	66.7	12.2
13	RSN960.eq	Canyon Country - W Lost Cany	6.69	124.0	0.4	44.4	11.3
14	RSN1003.eq	LA - Saturn St	6.69	27.0	0.4	41.6	5.0
15	RSN1077.eq	Santa Monica City Hall	6.69	26.5	0.9	41.6	15.2
16	RSN1107.eq	Kakogawa	6.9	22.5	0.3	26.9	8.8
17	RSN1116.eq	Shin-Osaka	6.9	19.2	0.2	31.3	8.4
18	RSN1158.eq	Duzce	7.51	15.4	0.3	58.9	44.1
19	RSN1203.eq	CHY036	7.62	16.0	0.2	44.8	34.0
20	RSN3749.eq	Fortuna Fire Station	7.01	20.4	0.3	38.1	16.7

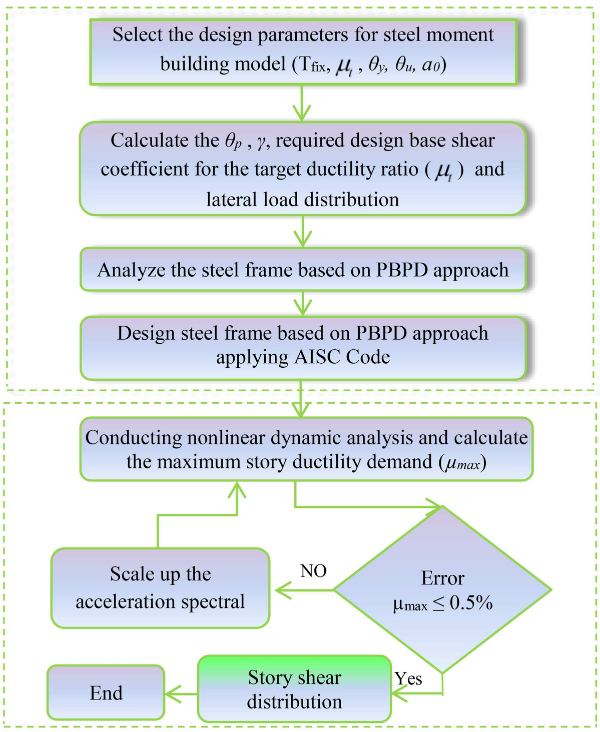

Figure 5. Flowchart showing a general procedure for Performance-Based Plastic Design (PBPB) approach to the constant-ductility nonlinear dynamic analysis of fixed- and flexible-base buildings.

Figure 6 shows relative story shear distributions obtained from nonlinear dynamic analyses of 4-, 8-, and 16-story fixed-base SMRFs that are designed by the conventional PBPD subjected to 20 individual earthquake ground motions. The results are provided at two levels of low and high inelastic behavior. In addition, the average results of all the selected ground motions along with shear force pattern having different shear proportional values are provided and compared. As seen earlier, the distribution power b is a function of the fundamental period of vibration and the level of inelastic behavior, such that it decreases and increases by increasing the period and ductility demand value, respectively. The dependency of the fundamental period is also reported and consistent with the previous studies [16,19]. However, nothing has been yet reported on the effect of the target ductility demand on the b value. The results of this figure show that the optimum b value could vary from 0.67 to 1.1 based on the values of T_{fix} and μ_t. The results are discussed in the upcoming section in greater detail.

6. Effect of shear proportional factor

Frames with 4-, 8-, 12-, and 16-story levels were used to find an optimal distribution of the shear proportioning factor through nonlinear dynamic analysis. Each frame was designed using four possible functions for the shear proportioning factor. These functions were assumed by the values of b taken as 1, 0.75, 0.5, and 0.25. The member sizes of the frame structures are designed by selecting 2% target drift and using the design parameters, as presented in the previous section. It was assumed that the distribution of beam strengths followed the distribution of shear proportioning factors. The results showed the relative distribution of maximum story

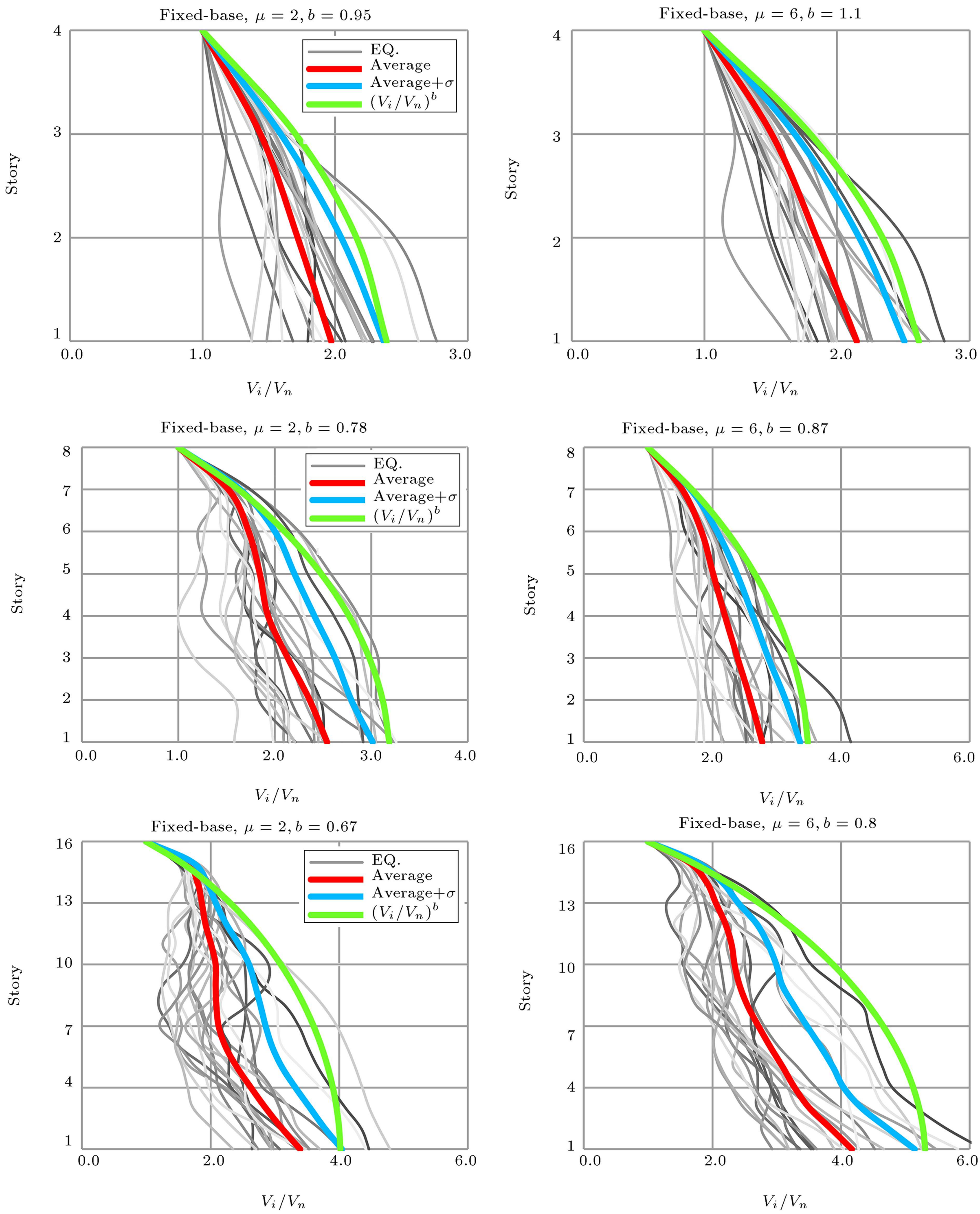

Figure 6. Relative distribution of story shear V_i/V_n for fixed-base structures under strong ground motions.

shears of the selected frames and the upper bound distribution of shear proportioning factors in the nonlinear dynamic analysis results for various ductility demands.

For a 4-story frame structure with a shorter period ($T = 0.72$ s) and regardless of the values of the shear proportioning factor, the relative distributions of maximum story shears are close together. The relative story shear distribution using various values of b ranging from 0.7 to 0.9 represents an upper bound of the nonlinear dynamic analysis results at low to high ductility ratios. As shown for the short-period frame structure, the required value of b increases considerably as the level of inelasticity increases. To achieve more realistic distributions of the shear proportioning factor according to the period of the structures under strong motions, results of 8-, 12-, 16-story building structures are provided. The relative distributions of maximum earthquake-induced story shears for each case of 8- to 16-story frames are shown in Figure 3. As shown earlier, the distribution of maximum earthquake-induced story shears of frames is related to the period and can be approximated using optimal b values of the shear proportioning factor at various levels of inelasticity. As illustrated earlier, the optimal b value decreases as the period increases, and it increases as the target ductility demand increases. Based on the mean results of the distribution of maximum story shears of frames obtained from 20 strong earthquakes, the optimal b value for each frame can be determined by the trend line at the upper bound of story shear distribution for various ductility demands. For an 8-story (T = 1.44 s) building, the optimal b value is obtained ranging from 0.65 to 0.7 for low to high ductility demands by calculating the least square fit values. Further analyses by Chao and Goel (2005 and 2006a) [41,42] showed that the relative story shear distribution using $b = 0.75$ represented an upper bound of the nonlinear dynamic analysis results. The same analysis was conducted in the case of the 12- and (T = 2.1 s) 16-story (T = 2.5 s) building frames with a longer period, and the corresponding values of b were then obtained at various ductility ratios. Consequently, the optimal b value for these cases and the recommended trend line for selected frames are presented in Figure 7.

7. Effect of ductility

The effects of ductility demand on the relative story shear demand distribution are investigated using three SMRF systems with 4, 8, 12, and 16 stories as representative of low- to high-rise buildings. Results of the relative distribution of story shear at various low to high levels of inelasticity ($\mu = 2, 4, 6$) are plotted in Figure 8. As demonstrated, generally, by increasing the level of inelasticity, the relative story shear increases for all models from shorter to long period cases. In the selected frames with various stories, a small difference of story shear can be seen between moderate and high levels of inelasticity ($\mu = 4, 6$) when compared with the corresponding value of low ductility demand. Further, it is revealed that this trend is followed for low- and high-rise SMRF buildings. The b value corresponding to lower and higher ductility demands are obtained based on the relative distributions of maximum story shears.

8. Effect of base flexibility

In order to examine the effect of soil flexibility on the nonlinear response of SMRFs designed based on the PBPD approach, Figure 9 is plotted. To this end, the individual, mean, mean plus standard deviation ($mean + \sigma$), and different shear proportion factors are shown at low ($a_0 = 1$) and high ($a_0 = 2$) levels of base flexibility. As seen, by increasing the a_0 value, the amount of the required parameter b decreases; however, in the case of predominant SSI effect ($a_0 = 2$), the relative story shear demands of top stories increase. In addition, as can be seen, the mean envelope curves of the maximum responses can adequately predict the required relative shear force demands of all the selected records that are obtained by changing the b values. In fact, for each soil-structure system, the optimum b values were computed based on nonlinear dynamic analyses. It is also observed that the envelope curves corresponding to the optimum values are very close to the curves of $+\sigma$. The results indicate that, similar to the fixed-base systems, the shear proportion factor b is dependent on both fundamental period and level of inelastic demands, where the latter effect has not been taken into account for the conventional PBPD approach. It can be observed that by increasing the structural period and ductility demand, the b values decrease and increase, respectively. Based on the optimum values of b, a practical expression is proposed in the next section.

9. Dispersion of results and proposed practical equation

The results presented in the previous sections are obtained from the mean responses of an ensemble of 20 strong ground motions listed in Table 2. It is clear that the application of the mean value provides an average, where its efficiency depends on the dispersion of computed results. Based on observations, it is believed that the structural response of a structural system with certain dynamic characteristics is strongly related to the selected ground motion record. In addition, the dispersion of results shows the impact of record-to-record variability on the nonlinear responses of systems. Hence, as an effective tool to evaluate the dispersion of obtained results, the Coefficient Of Variation (COV) is utilized, which is defined as the ratio of the standard deviation to the mean value. As illustrated in Figure 10, the COV distribution is provided for the 8- and 16-story SMRF structures with various ductility demands. The derived spectra present the dispersion along the height of selected models. It is observed that increasing the fundamental period of structures is accompanied by an increase in COV of the maximum story shear distribution in both fixed- and flexible-base cases. The COV values of the results exhibit low dependency on the ductility demand for structures with shorter periods. This is probably because the structural response is governed primarily

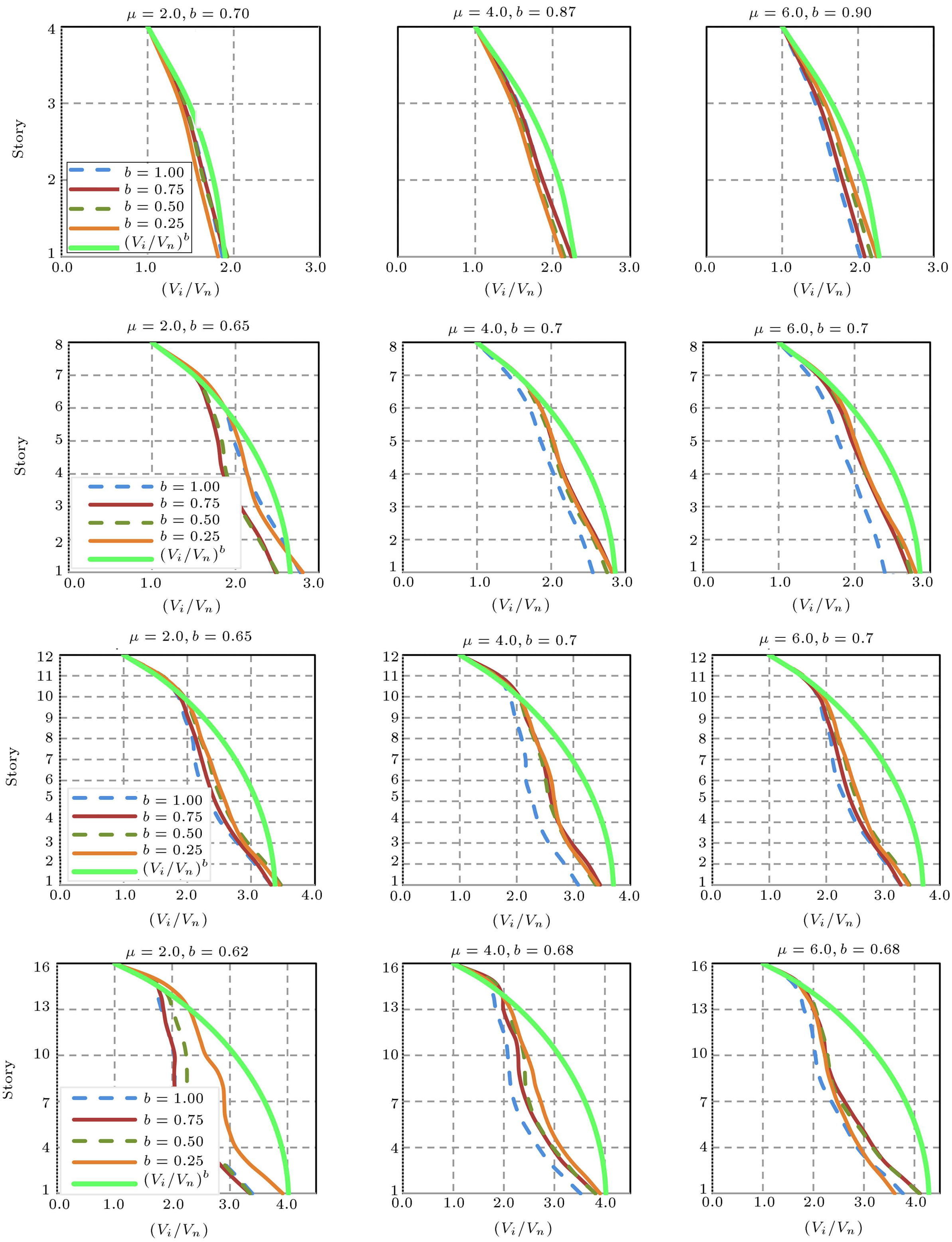

Figure 7. Comparison of relative shear distributions by various shear proportioning factors and fixed-base system.

by the fundamental vibration mode in a short period range; hence, the ductility demands along the building height also follow the fundamental mode pattern.

The format for this design lateral force distribution based on the inelastic state of a structure was originally proposed by Lee and Goel [16] by using the shear distribution factor derived from the relative distribution of maximum story shears of a large number of SMRFs subjected to four selected earthquake records. They applied the least square fit method and proposed

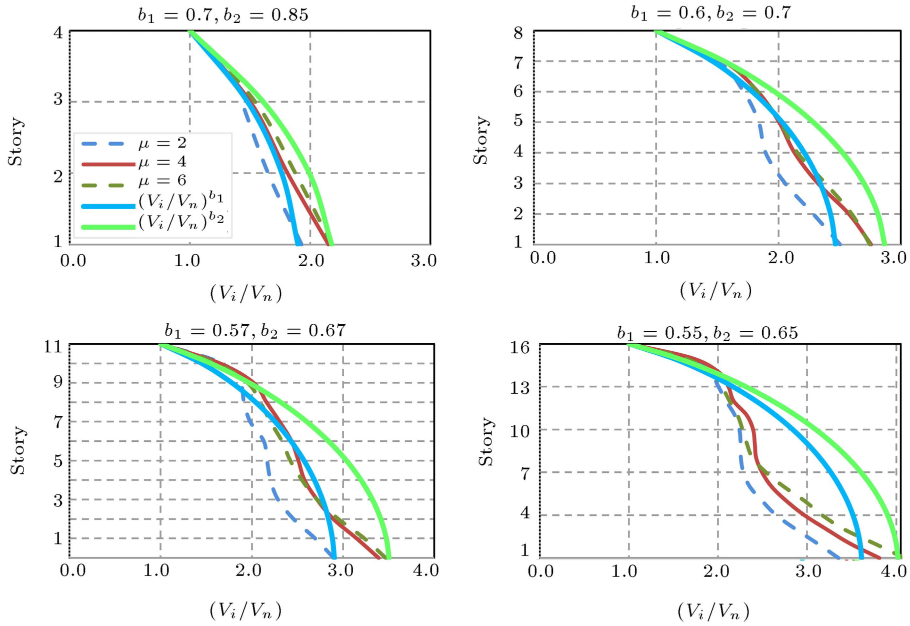

Figure 8. Relative distribution of story shear V_i/V_n for designed Moment Frames (MFs) with various ductilities.

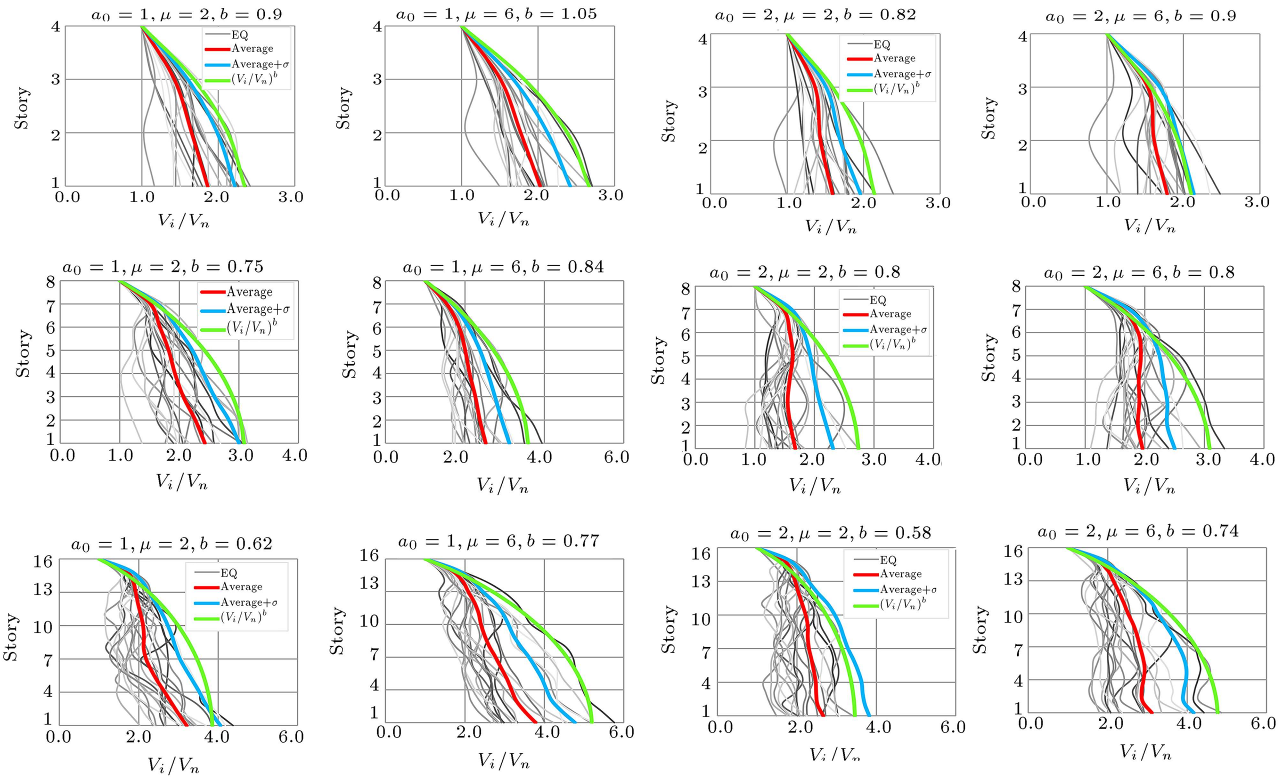

Figure 9. Relative distribution of story shear V_i/V_n for designed Moment Frames (MFs) for flexible-base Steel Moment-Resisting Frames (SMRFs).

practical Eq. (19), in which b is defined as Eq. (20):

$$b = \alpha T^{-0.2}. \tag{20}$$

T is the fundamental period. The value of parameter α was originally proposed as 0.5 by Lee and Goel (2001) [16], which was later revised to 0.75 based on more extensive nonlinear dynamic analyses of Eccentrically Braced Frames (EBFs) and Special Truss Moment Frames (STMFs) by Chao and Goel [41,42]. However, the level of inelastic behavior (i.e., ductility demand) was not considered in their proposed

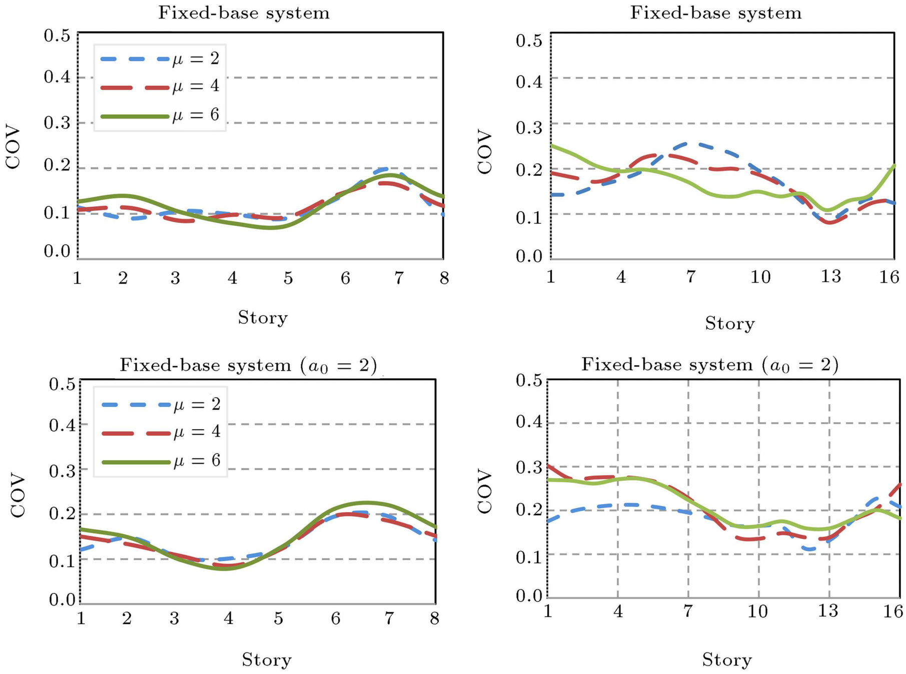

Figure 10. The Coefficient Of Variation (COV) of the relative distribution of story shear V_i/V_n for various ductility demands.

equation. In this study, extensive nonlinear dynamic analyses were carried out on SMRF systems designed based on the PBPD approach and at different levels of inelasticity (i.e., constant ductility demand) to modify the suggested lateral force distribution for various ductility demands. Based on the proposed equation for various ductility demands, a more realistic design lateral force distribution was obtained that accounts for the inelastic behavior of structures when subjected to strong ground motions. The suggested optimum b value for the lateral force distribution that can be applied to most of the conventional frame types is defined as Eq. (21):

$$b = aT^{-c}, \tag{21}$$

where the parameters a and c are computed from nonlinear regression analyses of numerical data for both fixed- and flexible-base structures having two levels of low and high inelastic behaviors, as shown in Figure 11. As can be seen, the proposed equations can adequately estimate the optimum values of b for both fixed-and (SSI) systems. In addition, the results clearly show that the optimum b value increases with increasing the ductility demand. Conversely, the b value decreases with increasing the a_0 parameter, while, similar to the fixed-base systems, it descends with increasing the fundamental period.

10. Conclusions

This study carried out extensive nonlinear dynamic analyses on fixed- and flexible-base Steel Moment-Resisting Frame (SMRF) systems designed based on a new constant-ductility Performance-Based Plastic Design (PBPD) approach at different levels of inelasticity under a group of 20 strong earthquake ground motions to modify the suggested lateral force distribution for various ductility demands. The effect of inertial soil-structure systems was parametrically investigated on the height-wise distribution of relative shear force demands. In addition, the adequacy of various lateral load patterns in ductility distribution of PBPD frame buildings was investigated. Based on the results, it was revealed that the height-wise distribution of story ductility demands tended to be more uniform as the fundamental period of the structure increased. However, by increasing the ductility ratios, the distribution of the ductility demand became more non-uniform along the height of the structure.

Based on the proposed equation for various ductility demands, a more realistic design lateral force distribution was proposed, accounting for the inelastic behavior of structures when subjected to strong ground motions. The suggested lateral force distribution can be applied to most of the conventional steel MF systems. The results showed that the suggested modification for lateral force distribution for the types of steel-framed structures investigated in this study was more rational and made a better prediction of inelastic seismic demands at various levels of inelasticity. It was demonstrated that the proposed equations could adequately estimate the optimum values of shear pro-

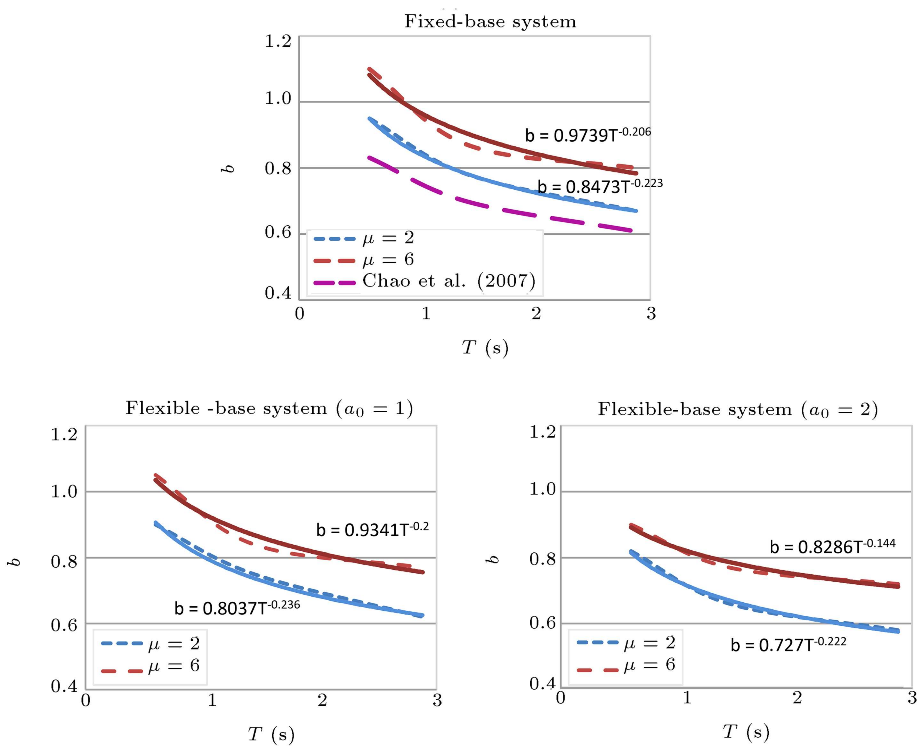

Figure 11. Optimum b values versus structure period for fixed and flexible Steel Moment-Resisting Frames (SMRFs), average of 20 earthquakes.

portioning factor b for both fixed and Soil-Structure Interaction (SSI) systems. In addition, the results clearly showed that optimum b value increased with increasing the ductility demand. Conversely, the b value decreased with increasing the a_0 parameter, while, similar to the fixed-base systems, it descended with increasing the fundamental period.

References

1. IBC ICC "International code council. International building code", International Code Council: Washington DC, United States (2012).
2. ASCE/SEI 7-05 "Minimum design loads for buildings and other structures", Reston (VA): American Society of Civil Engineers (2010).
3. Council, Building Seismic Safety "NEHRP recommended seismic provisions for new buildings and other structures (FEMA P-750)", Federal Emergency Management Agency, Washington, DC (2009).
4. Uniform Building Code In *International Conference of Building Officials*, Whittier, California, UBC (1997).
5. Anderson, J.C., Miranda, E., and Bertero, V.V., *Evaluation of the Seismic Performance of a Thirty-Story RC Building*, Berkeley: Earthquake Engineering Research Centre, University Of California, UCB/EERC-91/16 (1991).
6. Gilmore, T.A. and Bertero V.V., *Seismic Performance of a 30-story Building Located on Soft Soil and Designed According to UBC 1991*, Berkeley: Earthquake Engineering Research Center, University of California, UCB/EERC-93/04 (1993).
7. Chopra, A.K., *Dynamics of Structures-Theory and Applications to Earthquake Engineering*, 4th Edition, Englewood Cliffs, New Jersey: Prentice Hall (2012).
8. Leelataviwat, S., Goel, S.C., and Stojadinovic, B. "Toward performance-based seismic design of structures", *Earthq. Spectra*, **15**(3), pp. 435–461 (1999).
9. Mohammadi, K.R., El-Naggar M.H., and Moghaddam H. "Optimum strength distribution for seismic resistant shear buildings", *Int. J. Solids Struct.*, **41**(21–23), pp. 6597–6612 (2004).
10. Moghaddam, H. and Hajirasouliha, I. "Toward more rational criteria for determination of design earthquake forces", *Int. J. Solids Struct.*, **43**(9), pp. 2631–2645 (2006).
11. Hajirasouliha, I. and Moghaddam, H. "New lateral force distribution for seismic design of structures", *J. Struct. Eng.*, ASCE, **135**(8), pp. 906–15 (2009).
12. Hajirasouliha, I. and Pilakoutas, K. "General seismic load distribution for optimum performance-based design of shear-buildings", *J. Earthq. Eng.*, **16**(4), pp. 443–62 (2012).
13. Chopra, A.K., *Dynamics of Structures: Theory and Applications to Earthquake Engineering*, 2nd Ed., Prentice-Hall, London (2001).
14. Moghaddam, H., *Earthquake Engineering*, 1st Ed., RTRC, Tehran, Iran (in Persian) (1995).

15. Moghaddam, H. and Mohammadi, R.K. "More efficient seismic loading for multi-degrees of freedom structures", *J. Struct. Eng.*, **132**(10), pp. 1673–1677 (2006).

16. Lee, S.S. and Goel, S.C. "Performance-based design of steel moment frames using target drift and yield mechanism", Department of Civil and Environmental Engineering, University Of Michigan, Report no. UMCEE 01-17 (2001).

17. Goel, S.C., Liao, W.C., Reza Bayat, M., and Chao, S.H. "Performance-based plastic design (PBPD) method for earthquake-resistant structures: An overview", *Struct. Des. tall Spec. Build.*, **19**(1–2), pp. 115–137 (2010).

18. Park, K. and Medina R.A. "Conceptual seismic design of regular frames based on the concept of uniform damage", *J. of Struct. Eng.*, **133**(7), pp. 945–955 (2007).

19. Chao, S.H., Goel, S.C., and Lee, S.S. "A seismic design lateral force distribution based on inelastic state of structures", *Earthq. Spectra*, **23**(3), pp. 547–569 (2007).

20. Ghannad, M.A. and Jahankhah, H. "Site dependent strength reduction factors for soil-structure systems", *Soil Dyn Earthq. Eng.*, **27**(2), pp. 99–110 (2007).

21. Banihashemi, M.R., Mirzagoltabar, A.R., and Tavakoli, H.R. "Development of the performance based plastic design for steel moment resistant frame", *Int. J. of Steel Struct.*, **15**(1), pp. 51–62 (2015).

22. Aviles, J. and Perez-Rocha, J.L. "Use of global ductility for design of structure-foundation systems", *Soil Dyn. Earthq. Eng.*, **31**(7), pp. 1018–1026 (2011).

23. Ganjavi, B. and Hao, H. "Optimum lateral load pattern for seismic design of elastic shear-buildings incorporating soil-structure interaction effects", *Earthq. Eng. Struct. Dyn.*, **42**, pp. 913–933 (2013).

24. Bolourchi, S.A. "Optimum seismic design of shear-buildings with soil-structure interaction effects", MSc. thesis, Sharif University of Technology (2007).

25. Ganjavi, B. and Hao, H. "A parametric study on the evaluation of ductility demand distribution in multi-degree-of freedom systems considering soil-structure interaction effects", *Eng. Struct.*, **43**, pp. 88–104 (2012).

26. Ganjavi, B., Hajirasouliha, I., and Bolourchi, A. "Optimum lateral load distribution for seismic design of nonlinear shear-buildings considering soil-structure interaction", *Soil Dyn. Earthq. Eng.*, **88**, pp. 356–368 (2016).

27. Newmark, N.M. and Hall, W.J., *Earthquake Spectra and Design*, Earthquake Eng. Res. Inst., El Cerrito, California (1982).

28. AISC. AISC-341-10 "Seismic design provisions for steel structures", American Institute of Steel Construction (AISC), Chicago, IL (2010).

29. Wolf, J.P., *Foundation Vibration Analysis Using Simple Physical Models*, Englewood Cliffs, NJ: Prentice-Hall (1994).

30. Wolf, J.P. and Deeks, A.J., *Foundation Vibration Analysis: A Strength-of-Materials Approach*, Burlington, MA: Elsevier (2004).

31. FEMA 440. "Improvement of nonlinear static seismic analysis procedures", Report No. FEMA 440, Federal Emergency Management Agency, prepared by Applied Technology Council (2005).

32. Kramer, S.I., *Geotechnical Earthquake Engineering*, Englewood Cliffs, NJ, Prentice-Hall (1996).

33. Veletsos, A.S. "Dynamics of structure-foundation systems (a volume honoring N.M. Newmark)", In *Structural and Geotechnical Mechanics*, W.J. Hall, Ed., Englewood Cliffs, NJ, Prentice-Hall, pp. 333–361 (1977).

34. Stewart, J.P., Seed, R.B., and Fenves, G.L. "Seismic soil-structure interaction in buildings II: empirical findings", *J. Geo. Tech. Geo. Environ. Eng.*, ASCE, **125**(1), pp. 38–48 (1999).

35. Ghannad, M.A. and Jahankhah, H. "Site dependent strength reduction factors for soil- structure systems", *Soil Dyn. Earthq. Eng.*, **27**(2), pp. 99–110 (2007).

36. Ganjavi, B. and Hao, H. "Ductility reduction factor for multi-degree-of freedom systems with soil-structure interaction", *15th World Conference on Earthquake Engineering* (2012).

37. Mazzoni, S., McKenna, F., Scott, M.H., and Fenves, G.L. "Opensees, OpenSees command language manual", *Open System for Earthquake Engineering Simulation* (2011).

38. Ruiz-García, J. and González, E.J. "Implementation of displacement coefficient method for seismic assessment of buildings built on soft soil sites", *Eng. Struct.*, **59**, pp. 1–12 (2014).

39. FEMA-450 "NEHRP recommended provisions for new buildings and other structures", Federal Emergency Management Agency (2003).

40. Ganjavi, B., Hong Hao, and Hajirasouliha, I. "Influence of higher modes on strength and ductility demands of soil-structure systems", *J. Earthq. Tsunami*, **10**(4), 1650006 (2016).

41. Chao, S.-H. and Goel, S.C. "Performance-based seismic design of EBF using target drift and yield mechanism as performance criteria", Report No. UMCEE 05-05, Department of Civil and Environmental Engineering, University of Michigan, Ann Arbor (2005).

42. Chao, S.-H. and Goel, S.C. "Performance-based plastic design of seismic resistant special truss moment frames", Report No. UMCEE 06-03, Department of Civil and Environmental Engineering, University of Michigan, Ann Arbor (2006a).

Biographies

Abolfazl Gholamrezatabar is a PhD Student at Iran University of Science & Technology, Tehran, Iran.

His current research interests include structural seismic performance and seismic retrofitting.

Behnoud Ganjavi received his PhD degree in Earthquake and Structural Engineering from the University of Western Australia in January 2013. Now, he works as an Associate Professor of Earthquake Engineering at University of Mazandaran. His current research interests include earthquake engineering with an emphasis on dynamic soil-structure interaction and optimum performance-based seismic design.

Gholamreza Ghodrati Amiri received his PhD degree in Earthquake Engineering from McGill University, Montreal, Canada in 1997. Now, he works as a Full Professor and the Dean of School of Civil Engineering, Iran University of Science & Technology, Tehran, Iran. His current research interests include seismic performance, evaluation and retrofit of existing structures.

Mohsen Ali Shayanfar received his PhD degree in Earthquake Engineering from McGill University, Montreal, Canada, in 1997. Now, he works as an Associate Professor of School of Civil Engineering, Iran University of Science & Technology, Tehran, Iran. His current research interests include the reliability of structures and the retrofitting and repairing of structures, especially buildings and bridges.